Supplementary Information

pH-Controlled Electrodeposition of Diameter-Modulated Co Nanowires:

Crystal Texture and Magnetic Properties

Seyed-Majid Peighambari-Sattari[a,b,c], Farzad Nasirpouri[*a] and Manuel Vazquez[c]

a. Faculty of Materials Engineering, Sahand University of Technology, Tabriz, 51335-1996, Iran.

b. Department of Metallurgical and Materials Engineering, Faculty of Chemical Engineering and Advanced Materials, Urmia University of Technology, Urmia 57155-419, Iran

c. Institute of Materials Science of Madrid, CSIC, 28049 Madrid, Spain.

**-Corresponding author: nasirpouri@sut.ac.ir, f_nasirpouri@yahoo.com.*

Table SI- Summary of data provided in previous articles on homogeneous and modulated diameter cobalt nanowires prepared under different pH conditions.

Type	Geometry	pH	XRD Result	Magnetic properties	Reference
Homogeneous diameter Co nanowire	D = 380-420 nm L = 6-10 µm	3.6	In samples deposited without a magnetic field, strong peaks from the hcp Co (100), (002), and (101) planes are observed. Conversely, samples deposited under a perpendicular magnetic field exhibit only a strong (002) peak of hcp Co.	During fabrication with a perpendicular magnetic field, the c-axis of hcp-Co becomes perpendicular to the film plane, with both shape and magnetocrystalline anisotropies favoring magnetization along the wire axis. Conversely, an in-plane magnetic field promotes Co nanowire growth with the c-axis in the film plane, inducing weak in-plane anisotropy.	Ge, S., et al., 2001, [1]
Homogeneous diameter Co nanowire	D = 30-450 nm L = 10-20 µm	3.8	When the wire diameter is reduced below 50 nm, the preferential orientation of the crystal easy magnetization axis (c-axis) shifts from perpendicular to parallel relative to the wire axis.	For nanowires with small diameters, shape and magnetocrystalline anisotropies both favor magnetization alignment along the wire axis. In large-diameter nanowires, a longitudinal single-domain state is unattainable at zero field, where complex multidomain patterns with a strong transverse magnetization component consistently form.	Henry, Y., et al., 2001. [2]
Homogeneous diameter Co nanowire	D = 9-22 nm L = 10-1000 nm	3-4	--	Coercivity (Hc) increases steeply with increasing nanowire length until reaching a constant value.	D. Sellmyer, et al., 2001, [3]
Homogeneous diameter Co nanowire	D = 12-50 nm L = 10-1000 nm	--	--	As temperature decreases, the easy magnetization axis deviates from the wire's long axis. The presence of fcc-Co potentially reduces the net magnetocrystalline anisotropy strength.	P. Paulus, et al., 2001. [4]
Homogeneous diameter Co nanowire	D = 70 nm L < 22 µm	2 & 3.8	The wires are polycrystalline with an hcp structure, primarily composed of grains several microns in size. At high pH, a considerable proportion of grains have their c-axis aligned almost perpendicular to the wire axis, whereas decreasing pH favors deposition of disordered hcp Co grains.	Lowering pH decreases the magnetocrystalline anisotropy contribution, thereby increasing the effective anisotropy field while keeping the easy axis parallel to the wires. High-pH samples exhibit a higher saturation field, and the reduced remanence in such samples is consistent with a lowered anisotropy field along the wire axis.	Encinas, A., et al. 2002, [5]
Homogeneous diameter Co nanowire	D = 29 nm L < 22 µm	2 3.84	At pH = 4.0, only a (100) peak is detected, consistent with hcp Co nanowires exhibiting a strongly dominant c-axis perpendicular to the wire axis and no other phases. In contrast, at pH = 6.4, Co nanowires show a (002) peak with almost total suppression of the (100) peak,	At low pH (2.0), magnetic properties indicate no magnetocrystalline anisotropy (MCA) contribution. At high pH (above 6.0), the increased effective anisotropy aligns with Co grains having their c-axis oriented parallel to the wires.	Darques, M., et al., 2004. [6]

		6.4 6.6	indicating a preferred crystallographic orientation change of the c-axis toward the direction parallel to the wires.		
Homogeneous diameter Co nanowire	D = 29 nm L = 10-1000 nm	2 3.8 6.6	The plating current and pH of the sulfate bath, rather than the wire diameter, are the key parameters determining c-axis orientation in electrodeposited Co nanowires.	The lowest resonance field is measured in the pH = 6.6 sample, whereas the highest resonance field is observed in the pH = 3.8 sample.	M. Darques, et al., 2004, [7]
Homogeneous diameter Co nanowire	D = 70 nm L ≈ 2 μm	2.5 3-3.5 5	The crystal structure of Co nanowires is fcc at pH = 2.5, a mixed fcc/hcp at pH = 3.0 and 3.5, and hcp at pH = 5.0.	Along the wire axis, the FCC structure exhibits higher coercivity and squareness than the HCP structure.	F. Li, et al., 2004. [8]
Homogeneous diameter Co nanowire	D = 320 nm L = 8.1 μm	4.0	Cobalt grows in the hcp phase and exhibits a weak (110) texture.	The easy axis of the nanowires lies along the wire direction, with shape anisotropy dominating over intrinsic magnetocrystalline anisotropy.	Qin, J., et al., 2005, [9]
Homogeneous diameter Co nanowire	D = 50 nm L = --	2.5	Co nanowires possess the hcp structure with a preferred [100] orientation.	Co nanowires were fabricated under two magnetic field directions: parallel and perpendicular to the nanowires' long axis.	Pan, H., et al., 2005, [10]
Homogeneous diameter Co nanowire	D = 35, 45, 65 nm L = 18 μm	2-3	The cobalt nanowires are single crystals with a highly preferential orientation, which becomes more ideal as the nanowire diameter decreases.	The axis along the cobalt nanowires is easy to magnetize, while the perpendicular axis is hard.	Xu, J., et al., 2005, [11]
Homogeneous diameter Co nanowire	D = 40 nm L < 5 μm	2.5	At a pulse frequency of 25 Hz, monocrystalline hcp Co nanowires form with a well-defined [$10^{-}10$] growth axis along the wire length. At a higher frequency of 1000 Hz, fcc Co nanowires deposit with small grain size and a preferred [111] texture directed along the wire length.	Magnetic properties demonstrate that FCC Co nanowire arrays possess larger coercivity and squareness values compared to other phases.	Zhang, J., et al., 2007, [12]
Homogeneous diameter Co nanowire	D = 40 nm L = 40 μm	4 &2	Single crystal orientations are as follows: pH = 4 (1.5 V): HCP [$10^{-}10$]; pH = 4 (2.4 V): FCC [111]; pH = 2 (3 V): FCC [220].	The parallel coercivity gradually increases as nanowire orientation transitions from HCP [$10^{-}10$] to FCC [220] and finally to FCC [111].	Huang, et al., 2008. [13]
Homogeneous diameter Co	D = 80 nm L = 80 & 270	3.19	Co nanowires are predominantly hcp with a (100) texture.	--	Jung, J., et al., 2008, [14]

nanowire	nm, 2.6 µm				
Homogeneous diameter Co nanowire	D = 15-45 nm L = 1-50 µm	5.7	The Co nanowires are consisting of oriented polycrystals with a preferred (100) growth direction perpendicular to the substrate	--	Malferrari, L., et al., 2009. [15]
Homogeneous diameter Co nanowire	D = 50 & 120 nm L = --	4.5	For D = 50 nm: All samples exhibit an hcp polycrystalline structure with preferred orientations. At 20°C, relative intensities of (100), (002), and (110) reflections are nearly equal; at 40°C, a preferred [100] orientation with low (110) intensity appears; at 60°C, the (101) reflection emerges. For D = 120 nm: The (002) diffraction peak appears only at 20°C. At 40°C, the (101) reflection becomes the main peak, while a preferred (100) orientation is obtained at 60°C electrolyte temperature.	All easy magnetization axes are oriented along the nanowire long axis.	Han, X., et al. 2009, [16]
Homogeneous diameter Co nanowire	D = 20-120 nm L = 5 µm	4.5-6.7	For D = 20 nm: The main peak is hcp Co (100). The (101) peak appears when the electrolyte pH reaches 6.4, and its intensity increases at pH 6.7. For D = 50 nm: At pH 4.5, three diffraction peaks correspond to hcp Co (100), (002), and (110). At pH 6.4, three peaks are observed: (100), (002), and (101). The (002) peak intensity increases rapidly with rising pH. For D = 120 nm: A single (002) diffraction peak is observed at pH 4.5, whereas (100) and (101) peaks are obtained at pH 6.7.	Coercivity increases markedly with rising pH, indicating that for diameters of 20 and 50 nm, coercivity is influenced by the (101) and (002) textures. No apparent magnetic anisotropy is observed in the 120 nm diameter sample.	Y. Ren, et al., 2009. [17]
Homogeneous diameter Co nanowire	D = 50 nm L = 6 µm	3.5	Diffraction patterns correspond to hcp and fcc polycrystalline reflections from Co (100), (111), (101), (200), and (220).	The magnetic properties of cobalt nanowires are dominated by magnetocrystalline anisotropy over shape anisotropy, attributed to a mixed fcc/hcp phase with preferential orientation near the perpendicular direction of the wire axis.	V. S. Rani, et al., 2009. [18]
Homogeneous diameter Co nanowire	D = 30 & 50 nm L = 3-6 µm	4.5	Nanowires with 30 nm diameter exhibit a diffraction pattern dominated by a highly textured Co-fcc phase oriented along [111] and [200]. Nanowires with 50 nm diameter show a more complex pattern, indicating a mixture of Co-hcp and Co-fcc phases.	Shape anisotropy contributions dominate the magnetic properties of fabricated Co nanowire arrays, exceeding the effects of magnetocrystalline anisotropy, magnetoelastic effects, and dipolar interactions among nanowires.	J. Sánchez-Barriga, et al., 2009. [19]
Homogeneous diameter Co nanowire	D =50, 65, 90 nm L = 30 µm	5	The Co nanowires have a hcp structure with a highly preferential orientation along the [1010] direction.	Owing to their cylindrical shape, the nanowires exhibit perpendicular anisotropy with the easy magnetization axis parallel to the Co nanowire axis. Both coercivity and Mr/Ms decrease with increasing wire diameter.	Yang, Y., et al. 2010, [20]

Modulated diameter Co nanowire	D = 70 & 110 nm L ≈ 4.7 µm	--	Cobalt nanowires show evidence of polycrystalline nanowires with highly crystalline regions. XRD reveals (101) and (100) directions of the hcp structure. In contrast, Co nanowires grown in a Mi-AAO template exhibit a strong (100) orientation.	Hysteresis loop squareness increases with higher aspect ratio and greater interpore distance. Coercivity also rises with aspect ratio but shows a distinct variation with interpore distance.	Lim, J.-H., et al., 2010. [21]
Homogeneous diameter Co nanowire	D = 35 nm L = 120-1000 nm	4	For longer wires, a strong preferential texture in the [100] directions of the hcp phase are observed, which increases with nanowire length. A change in preferred crystalline structure occurs from fcc cubic to hcp hexagonal in low- and high-aspect-ratio nanowires, respectively.	Short fcc-phase nanowires are dominated by shape anisotropy, in contrast to long nanowires.	Vivas, L., et al., 2011, [22]
Homogeneous diameter Co nanowire	D = 30 nm L = 1 µm	4-6	As acidity increases from pH 4 to 4.75, the (100) peak disappears, and the (101) peak intensity reaches a minimum at pH 5.25. Further increase in acidity causes the (100) and (110) peaks to reappear.	Coercivity and squareness are functions of electrolyte pH: they initially increase with acidity, reach a maximum, and subsequently decline.	A. Ramazani, et al., 2012. [23]
Homogeneous diameter Co nanowire	D = 50 nm L = 3 µm L = 30 µm	3.5 5.0 6.7	Strong textures along [100], [101], and [002] directions are observed for L = 3 µm. Increasing wire length leads to a reduction in crystal texture, particularly for the (002) peak.	Nanowires textured along the [002] crystallographic direction exhibit clear uniaxial magnetic anisotropy. [101]-textured nanowires show deviation of the easy axis from the wire axis, while [100] texture suggests a more complex anisotropy distribution.	Vivas, L., et al 2012, [24]
Homogeneous diameter Co nanowire	D = 100 nm L = 6 µm	4.5	The c-axis of the cobalt hexagonal structure is randomly oriented relative to the nanowire axis at 25°C, changes to a perpendicular direction at 50°C, and then becomes nearly parallel to the nanowire axis at 60°C.	--	Kaur, D., et al., 2012, [25]
Homogeneous diameter Co nanowire	D = 40 nm L = 10 µm	5	The nanowires are single crystals, with three peaks corresponding to diffraction from the (100), (002), and (101) planes of the hcp structure.	The easy axis of magnetocrystalline anisotropy is not parallel to that of shape anisotropy.	Ivanov, Y.P., et al., 2013, [26]
Homogeneous diameter Co nanowire	D = 40 nm L = 3-7 µm	3.5 5 6	At pH = 3.5, the strongest diffraction peak is the {100} reflection of hcp Co. At pH = 6.0, the strongest peak is the {101} reflection. At intermediate pH = 5.0, both {100} and {101} peaks are visible.	For wires grown at pH = 3.5, the parallel hysteresis loop shows low remanence and coercivity, indicating that magnetocrystalline anisotropy counterbalances shape anisotropy. With increasing pH, both remanence and coercivity rise notably; coercivity first increases with pH, then decreases after pH 6.0.	Ivanov, Y.P., et al., 2014, [27]
Periodical DM Co nanowire	D = 26-55 nm L = 50-60 µm	4.5	The polycrystalline structure remains similar, and the orientation parameter indicates a slight increase in crystal orientation for modulated nanowires.	Strong local stray fields at the ends of wider segments in modulated nanowires enhance magnetostatic interactions between neighboring nanowires. Straight nanowires exhibit a single magnetization process with enhanced uniaxial	Minguez-Bacho, I., et al., 2014 [28]

				longitudinal anisotropy.	
Homogeneous diameter Co nanowire	D = 250 nm L = 4-6 µm	8	The nanowires exhibit double texturing in the [111] (fcc) + [001] (hcp) directions. The hcp c-axis and the fcc [111] are both textured perpendicular to the nanowire long axis.	Magnetic domain configurations of individual nanowires (length 4–6 µm) reveal a spatial magnetization modulation along their length, which is length-dependent.	Arshad, M.S., et al., 2014, [29]
Homogeneous diameter Co nanowire	D = 95 nm L = 240 nm-5.75 µm	5.8	Several large grains (200–300 nm) are observed with the [0001] c-axis lying nearly perpendicular to the nanowire long axis.	--	Cantu-Valle, J., et al., 2015, [30]
Homogeneous diameter Co nanowire	D = 50 nm L = 8-15 µm	2 6.3 6.5	Polycrystal with main XRD peaks: pH = 2 → FCC (220); pH = 6.3 → HCP (101), (100); pH = 6.5 → HCP (002), (100).	This work presents a pathway for analyzing and simulating the static and dynamic properties of complex magnetic nanosystems exhibiting nontrivial magnetic behavior, relevant for developing wideband microwave applications under zero applied bias field conditions.	M. Pasquale, et al., 2023, [31]
Homogeneous diameter Co nanowire	D = 233 nm L = 3.82 µm	4.5	No specific preferential texture was observed in the X-ray diffraction patterns	Magnetocrystalline anisotropy is predominantly oriented parallel to the longitudinal axis of the nanowires.	T. R. Rakhmatullaev, et al., 2025, [32]

XRD analysis and further clarification

The X-ray diffraction (XRD) results have been reformatted to improve clarity and interpretation in Figure S1 As shown in the table below, the intensity of this peak does not exhibit any significant variation with changes in pH, indicating that it is not substantially affected by pH conditions.

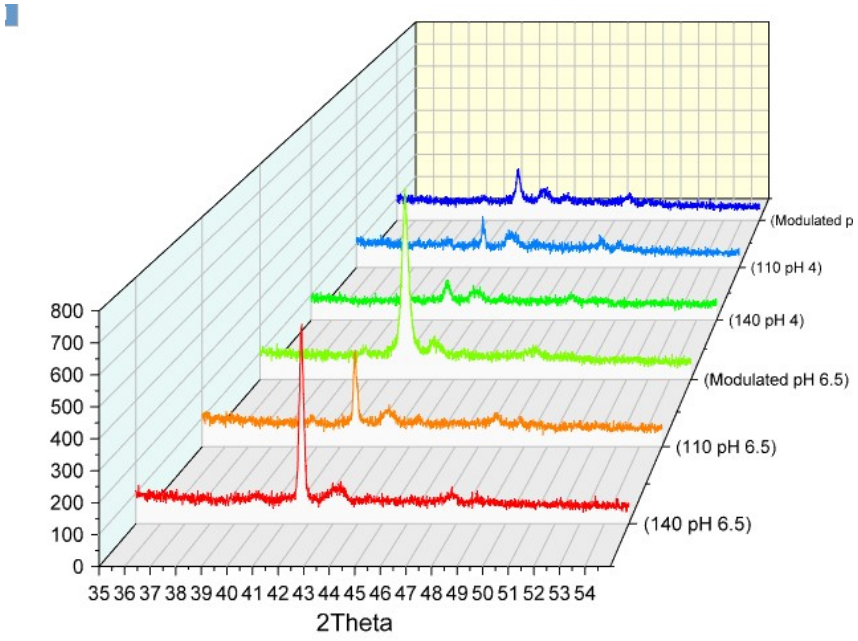

Figure S1 Reformated XRD pattern for DM nanowires, D=110 nm and D=140 nm homogeneous diameter nanowires at pH 4.0 and for DM nanowires, D=110 nm and D=140 nm homogeneous diameter nanowires at pH 6.5.

In addition, previous studies have reported the appearance of similar peaks associated with different substrate elements, including Au [27], Cu [32], Al and aluminum oxide [33, 34], and Ag [14]. Therefore, it is possible that one of the first four elements, or even an overlap of several contributions, may be responsible for the observed peaks in the present samples. For further clarification, this table has now been added to the Supplementary Information document.

Table SII - The intensity of peak * measured for different samples of Co NWs from XRD patterns.

Sample name	**Intensity of * peak ~**
MD pH 4	145
D110 pH 4	152
D140 pH 4	139
MD pH 6.5	153
D110 pH 6.5	148
D140 pH 6.5	138

Magnetic Force Microscopy imaging of the nanowires

In order to image individual nanowires, the alumina membrane was solved chemically and the nanowires were separated in ethanol by centrifugal force until receiving isolated individual nanowires. Figure S2 shows the MFM images of diameter modulated nanowires for both pH 4 and 6.5. The images show different magnetic contrast along the length of the nanowires with an approximate length below one micrometre. Each section of the nanowires contains two opposite magnetic contrasts in the crossover direction, which is in accordance with the curvature of the configuration of spins on the nanowire surface. These images suggest the existence of a multi vortex structure of periodic chirality along the nanowire. In the segments with smaller diameter, due to a smaller length, MFM images are slightly different from the larger segments. In the part where the diameter is reduced, the periodic chirality is stopped, and dark magnetic contrast is observed continuously.

From the MFM images we can assume that the magnetocrystalline anisotropy overcomes the shape anisotropy, and the sections associated with each vortex that change along the nanowire length, would vary in the length of every nanowire. The nanowire grown in pH 6.5 shows a more complex domain patterns, likely due to the competition between the shape and magnetocrystalline anisotropies.

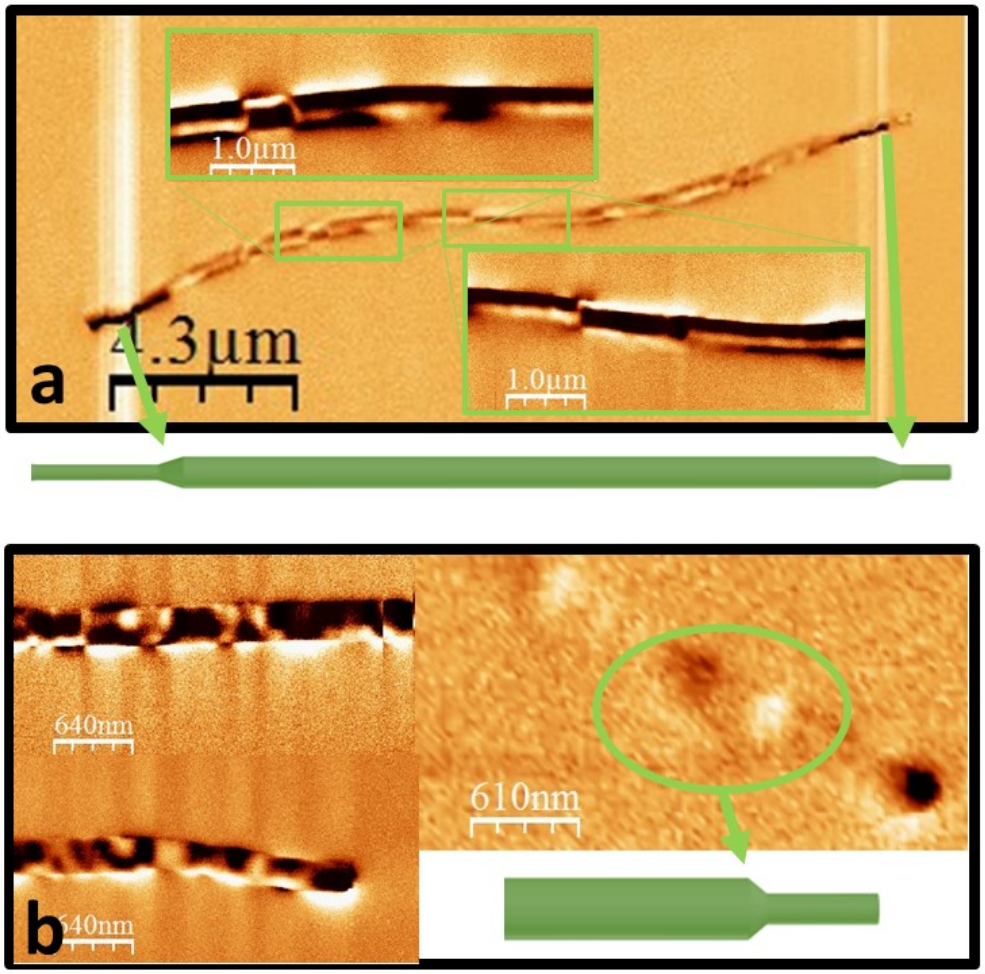

Figure S2 MFM image of Co modulated nanowire prepared in pH 4.0 (a) and pH 6.5 (b).

Calculation of the demagnetizing factor (Nz)-

The demagnetizing factor is calculated through the hypergeometric function, F, equation [35, 36]:

$$N_z(l) = 1 - F_{21}\left[\frac{4R^2}{l^2}\right] + \frac{8R}{3\pi l} \text{ where } F_{21}[x] = F_{21}[-1/2,1/2,2,-x]$$

according to:

$$F_{21}(a,b,c,x) = \sum_{n=0}^{\infty} \frac{(a)_n (b)_n x^n}{(c)_n \quad n!}$$

by:

$$(q)_n = \begin{cases} 1 & n = 0 \\ q(q+1)\ldots(q+n-1) & n > 0 \end{cases}$$

The Table SII summarizes the measured geometrical parameters of electrodeposited homogeneous and 4-segmented diameter modulated Co nanowires and corresponding demagnetizing factor N_z calculated individually for every segment of the nanowires. N_z is decreasing by increasing of the aspect ratio (L/D). Furthermore, the value of N_z becomes close to null for nanowires having infinite aspect ratio, where L/D>>0.

Table SIII Measured geometrical parameters (Length, L, and Diameter, D) of electrodeposited nanowires and calculated demagnetizing factor Nz for homogeneous and segments of the DM nanowires.

Nanowire Type		L(um)	D(um)	Nz
Homogeneous pH 4.0 140		22.6	0.14	0.0026
Homogeneous pH 4.0 110		44.8	0.11	0.0010
Homogeneous pH 6.5 140		8.2	0.14	0.0072
Homogeneous pH 6.5 110		17.5	0.11	0.0027
DM pH 4.0	Segment 1	0.7	0.11	0.0667
	Segment 2	13.9	0.14	0.0043
	Segment 3	2.5	0.11	0.0187
	Segment 4	14.1	0.14	0.0042
DM pH 6.5	Segment 1	0.8	0.11	0.0584
	Segment 2	7.2	0.14	0.0083
	Segment 3	1.8	0.11	0.0259
	Segment 4	11	0.14	0.0054

References:

1. Ge, S., et al., *Approach to fabricating Co nanowire arrays with perpendicular anisotropy: Application of a magnetic field during deposition.* Journal of Applied Physics, 2001. **90**(1): p. 509-511.
2. Henry, Y., et al., *Magnetic anisotropy and domain patterns in electrodeposited cobalt nanowires.* The European Physical Journal B-Condensed Matter and Complex Systems, 2001. **20**(1): p. 35-54.
3. Sellmyer, D., M. Zheng, and R. Skomski, *Magnetism of Fe, Co and Ni nanowires in self-assembled arrays.* Journal of Physics: Condensed Matter, 2001. **13**(25): p. R433.
4. Paulus, P., et al., *Low-temperature study of the magnetization reversal and magnetic anisotropy of Fe, Ni, and Co nanowires.* Journal of Magnetism and Magnetic Materials, 2001. **224**(2): p. 180-196.
5. Encinas, A., et al., *Effect of the pH on the microstructure and magnetic properties of electrodeposited cobalt nanowires.* IEEE Transactions on Magnetics, 2002. **38**(5): p. 2574-2576.
6. Darques, M., et al., *Controlled changes in the microstructure and magnetic anisotropy in arrays of electrodeposited Co nanowires induced by the solution pH.* Journal of Physics D: Applied Physics, 2004. **37**(10): p. 1411.
7. Darques, M., et al., *Tailoring of the c-axis orientation and magnetic anisotropy in electrodeposited Co nanowires.* Journal of Physics: Condensed Matter, 2004. **16**(22): p. S2279.
8. Li, F., et al., *Fabrication and magnetic properties of Co nanowire arrays of different crystal structures.* Chinese Science Bulletin, 2004. **49**(14): p. 1532-1535.
9. Qin, J., et al., *Differences in the magnetic properties of Co, Fe, and Ni 250− 300 nm wide nanowires electrodeposited in amorphous anodized alumina templates.* Chemistry of materials, 2005. **17**(7): p. 1829-1834.
10. Pan, H., et al., *Growth of single-crystalline Ni and Co nanowires via electrochemical deposition and their magnetic properties.* The Journal of Physical Chemistry B, 2005. **109**(8): p. 3094-3098.
11. Xu, J., et al., *Fabrication and magnetic property of monocrystalline cobalt nanowire array by direct current electrodeposition.* Materials letters, 2005. **59**(8-9): p. 981-984.
12. Zhang, J., et al., *Monocrystalline hexagonal-close-packed and polycrystalline face-centered-cubic Co nanowire arrays fabricated by pulse dc electrodeposition.* Journal of Applied Physics, 2007. **101**(5).
13. Huang, et al., *Orientation-controlled synthesis and ferromagnetism of single crystalline Co nanowire arrays.* The Journal of Physical Chemistry C, 2008. **112**(5): p. 1468-1472.
14. Jung, J., et al., *Fabrication and magnetic properties of Co nanostructures in AAO membranes.* Bulletin of the Korean Chemical Society, 2008. **29**(4): p. 758-760.
15. Malferrari, L., et al., *Alumina Template-Dependant Growth of Cobalt Nanowire Arrays.* Journal of Nanotechnology, 2009. **2009**: p. 8.

16. Han, X., et al., *Influence of crystal orientation on magnetic properties of hcp Co nanowire arrays.* Journal of Physics D: Applied Physics, 2009. **42**(9): p. 095005.
17. Ren, Y., et al., *The effect of structure on magnetic properties of Co nanowire arrays.* Journal of Magnetism and Magnetic Materials, 2009. **321**(3): p. 226-230.
18. Rani, V.S., et al., *Structural and magnetic properties of electrodeposited cobalt nanowires in polycarbonate membrane.* physica status solidi (a), 2009. **206**(4): p. 667-670.
19. Sánchez-Barriga, J., et al., *Interplay between the magnetic anisotropy contributions of cobalt nanowires.* Physical Review B, 2009. **80**(18): p. 184424.
20. Yang, Y., et al., *Diameter-controllable magnetic properties of Co nanowire arrays by pulsed electrodeposition.* Journal of Nanomaterials, 2010. **2010**: p. 3.
21. Lim, J.-H., et al., *Synthesis of mild–hard AAO templates for studying magnetic interactions between metal nanowires.* Journal of Materials Chemistry, 2010. **20**(41): p. 9246-9252.
22. Vivas, L., et al., *Coercivity of ordered arrays of magnetic Co nanowires with controlled variable lengths.* Applied Physics Letters, 2011. **98**(23): p. 232507.
23. Ramazani, A., M.A. Kashi, and G. Seyedi, *Crystallinity and magnetic properties of electrodeposited Co nanowires in porous alumina.* Journal of Magnetism and Magnetic Materials, 2012. **324**(10): p. 1826-1831.
24. Vivas, L., et al., *Magnetic anisotropy in ordered textured Co nanowires.* Applied Physics Letters, 2012. **100**(25): p. 252405.
25. Kaur, D., D.K. Pandya, and S. Chaudhary, *Texture changes in electrodeposited cobalt nanowires with bath temperature.* Journal of The Electrochemical Society, 2012. **159**(12): p. D713-D716.
26. Ivanov, Y.P., et al., *Magnetic structure of a single-crystal hcp electrodeposited cobalt nanowire.* EPL (Europhysics Letters), 2013. **102**(1): p. 17009.
27. Ivanov, Y.P., et al., *Crystallographically driven magnetic behaviour of arrays of monocrystalline Co nanowires.* Nanotechnology, 2014. **25**(47): p. 475702.
28. Minguez-Bacho, I., et al., *Electrochemical synthesis and magnetic characterization of periodically modulated Co nanowires.* Nanotechnology, 2014. **25**(14): p. 145301.
29. Arshad, M.S., et al., *Effect of magnetocrystalline anisotropy on the magnetic properties of electrodeposited Co–Pt nanowires.* Journal of nanoparticle research, 2014. **16**(11): p. 2688.
30. Cantu-Valle, J., et al., *Mapping the magnetic and crystal structure in cobalt nanowires.* Journal of applied physics, 2015. **118**(2).
31. Pasquale, M., et al., *Micromagnetic simulation of electrochemically deposited Co nanowire arrays for wideband microwave applications.* Journal of Physics D: Applied Physics, 2023. **56**(48): p. 485001.
32. Rakhmatullaev, T.R., et al., *Substrate-induced reorientation of the effective anisotropy in cylindrical Co and segmented Co/CoW nanowires.* Journal of Alloys and Compounds, 2025. **1044**: p. 184336.
33. Pirota, K.R. and M. Vazquez, *Arrays of electroplated multilayered Co/Cu nanowires with controlled magnetic anisotropy.* Advanced Engineering Materials, 2005. **7**(12): p. 1111-1113.
34. Garcıa, J., et al., *Magnetic behavior of an array of cobalt nanowires.* Journal of Applied Physics, 1999. **85**(8): p. 5480-5482.
35. Landeros, P., et al., *Scaling relations for magnetic nanoparticles.* Physical Review B—Condensed Matter and Materials Physics, 2005. **71**(9): p. 094435.

36. Beleggia, M., et al., *On the computation of the demagnetization tensor for particles of arbitrary shape.* Journal of Magnetism and Magnetic Materials, 2004. **272**: p. E1197-E1199.